Projektowanie, badania i eksploatacja
Designing, researches and exploitation
Engineer of XXI Century'2024

Comprehensive Assessment of Materials for 4D printing in Medical Implant Application

Piotr Szczygieł [1], Roman Novotný [2], Anna Kurowska [1], Jarosław Janusz [1], Adam Jabłoński [1], Jana Frankova [2], Izabella Rajzer [1]

[1] *University of Bielsko-Biala, Willowa 2, Bielsko-Biała 43-309, Poland, irajzer@ubb.edu.pl*
[2] *Palacký University Olomouc, Department of Medical Chemistry and Biochemistry, Hněvotínská 3, Olomouc 779 00, Czech Republic, roman.novotny@upol.cz*

Abstract: This article describes studies involving the use of 4D printing technology in medical applications. For this purpose, a drug-modified shape memory material was developed, specifically designed for the production of filaments for 4D printing of medical implants. Research has been carried out to assess material composition, biocompatibility, cells proliferation rate and shape memory properties.

Keywords: Biocompatibility, Cells, Shape Memory Polymers, 4D Printing, Implants

Kompleksowa ocena materiałów do druku 4D w zastosowaniu do implantów medycznych

Piotr Szczygieł [1], Roman Novotný [2], Anna Kurowska [1], Jarosław Janusz [1], Adam Jabłoński [1], Jana Frankova [2], Izabella Rajzer [1]

[1] *University of Bielsko-Biala, Willowa 2, Bielsko-Biała 43-309, Poland, irajzer@ubb.edu.pl*
[2] *Palacký University Olomouc, Department of Medical Chemistry and Biochemistry, Hněvotínská 3, Olomouc 779 00, Czech Republic, roman.novotny@upol.cz*

Streszczenie: Artykuł opisuje badania dotyczące zastosowania technologii druku 4D w medycynie. W tym celu opracowano modyfikowany lekami materiał z pamięcią kształtu zaprojektowany specjalnie do produkcji filamentu do druku 4D implantów medycznych. Przeprowadzono badania oceniające skład materiału, biokompatybilność, szybkość proliferacji komórek oraz właściwości pamięci kształtu.

Słowa Kluczowe: Biokompatybilność, komórki, polimery z pamięcią kształtu, druk 4D, implanty, leki

1. Introduction

4D printing represents an advanced evolution of 3D printing technology, enabling the fabrication of objects that can change their shape, properties, or function over time in response to specific environmental stimuli [1-3]. This temporal transformation is achieved through the use of shape memory polymers (SMPs), which are engineered to respond predictably to stimuli like temperature, moisture, or pH [4-5]. SMPs are characterized by their ability to switch between two configurations: a temporary shape and a permanent shape. When deformed into a temporary configuration, SMPs remain in this state until exposed to an external stimulus that activates their return to a predefined, permanent shape. Structurally, SMPs typically consist of two phases: (1) switching segments that temporarily "locks" the material in the deformed shape, and (2) stable segments that facilitate the material's recovery to its original shape upon stimulation.

DOI: https://doi.org/10.53052/9788367652261.12

The programmable shape-shifting properties and biocompatibility of SMPs make them highly suitable for developing adaptive, patient-specific implants via 4D printing [6-7]. This technology holds significant promise for medical applications where implants must conform to the dynamic anatomical environment, thereby improving integration with host tissues and reducing the need for additional surgical interventions. Polyglycolide and its copolymers with lactide and caprolactone are increasingly used in medical applications due to their biocompatibility and favorable mechanical properties. These materials are becoming more common for biodegradable implants, particularly in bone surgery where they are used for screws, plates, and scaffolds preparation [8-9].

In this study, we developed a drug-modified SMP material specifically designed for the production of filaments for 4D printing of medical implants. Microscopic observations were performed to assess the microstructure and evaluate the integration of the drug within the material matrix, while Fourier-transform infrared spectroscopy (FTIR) analyses were conducted to confirm the presence of the drug. Cell culture studies were performed to evaluate the biocompatibility of the developed materials. A study investigated the impact of drug addition on the material's ability to return to its defined, permanent shape.

This novel application of SMP materials in 4D printing paves the way for the next generation of responsive medical devices, with the potential to improve patient outcomes and advance minimally invasive therapeutic strategies.

2. Materials and Methods

The research was carried out on disc-shaped samples produced in the Laboratory of Biomaterials and Special Materials at the University of Bielsko-Biala. The polymer melting method was used. The materials for testing were obtained from a mixture of poly(lactide-co-glycolide-co-caprolactone) terpolymer and osteogenon drug (OST, PIERRE FABRE) [10] with a content of 95 wt.% TER and 5 wt.% OST. A segmental terpolymer of L-lactide, ε-caprolactone, and glycolide (L LA/GL/ε-CL 69/16/15) was synthesized in Centre for Polymer Materials of the Polish Academy of Sciences through ring-opening polymerization using zirconium acetylacetonate as a biocompatible initiator. The weighed polymer was mechanically mixed with OST particles and then homogenized at an elevated temperature (190°C). The process of forming blends was carried out by rolling plastic material. Using cutters, discs with a diameter of 0.6 cm and 1.2 cm were cut, corresponding to the diameters of the wells in the cell culture plate. For comparison, samples of pure terpolymer were also prepared. To test the shape memory ability, samples measuring 50x5.5x1.45 mm were made by rolling the material and then cutting the samples. The samples formed into a temporary shape (U) were immersed in distilled water at a temperature of 36.9 ◎C and the process of returning (deforming) the samples to their original shape was recorded.

Using an optical microscope (Opta-Tech, Poland) equipped with a CMOS 3 camera and OptaView IS software, the microstructure of the materials were assessed. Morphological observations were also conducted using a scanning electron microscope (Apreo 2 S LoVac, Thermo Fisher Scientific, Waltham, MA, USA) with the Octane Elect X-ray microanalysis system (EDAX Ametek GmbH Tilburg, the Netherlands). The samples were mounted on conductive carbon tape and sputter-coated with a 10 nm carbon layer (EM ACE600 sputter coater, Leica Microsystems, Wetzlar, Germany). Imaging was performed at an accelerating voltage of 10-18 kV under low vacuum, using secondary electron detection mode. FTIR spectra were recorded in the wavenumber range of 400–4000 cm^{-1} using a Thermo Scientific Nicolet iS5 FT-IR Spectrometer equipped with an iD7 ATR module and a diamond crystal for Attenuated Total Reflectance (ATR), with 32 scans at a resolution of 4 cm^{-1}.

Chemicals, Materials and Cells

Saos-2 cell line from ECACC (European Collection of Authenticated Cell Cultures, United Kingdom; Cat. No. 89050205). McCoy's 5A culture medium: Sigma-Aldrich, United States (Cat. No. M9309). Fetal Bovine Serum (FBS). Penicillin-streptomycin mixture: Sigma-Aldrich, United States, Cat. No. P4333. Phosphate buffer saline (PBS). Trypsin/EDTA: Thermo Fischer Scientific, United States (Cat. No. 25200-056). MTT (3-(4,5-dimethylthiazol-2-yl)-2,5-diphenyltetrazolium bromide), Sigma-Aldrich, United States, Cat. No. 57360-69-7. DMSO (Penta chemicals unlimited, Czech Republic, Cat. No. 67-68-5), NH3 (Penta chemicals unlimited, Czech Republic, Cat. No. 02096013). Acridine orange (P-LAB, Czech Republic, Cat. No. 46005).

Cultivation of Saos-2 cells

Saos-2 cells were cultured in McCoy's 5A medium supplemented with 10 % FBS and penicillin-streptomycin at 37°C with 5% CO2. Once cells reached 80% of confluence, they were subcultured. The original culture medium was discarded, and the cells were washed twice with 15-20 ml PBS. Trypsin/EDTA was added, and the flask was incubated (37 ˚C, 5% CO2) for 2-3 minutes, until the cells detached from the bottom of cultivation flask. After cell detachement, culture medium with serum was added to neutralize the trypsin. The cell suspension was centrifuged at 1000 rpm for 3 minutes at RT. The suspension of the cells was discarded, and the cell pellet was resuspended in 5 ml of fresh culture medium. The cell suspension was either transferred to new culture flasks or counted and seeded onto culture plates.

Sterilization of materials

All tested materials were sterilized by immersion in 70% ethanol for 24 hours, followed by UV irradiation for 20 minutes on each side.

Table 1: tested materials

Material title	Additive
TER_OST_5_BL	Ostegenon
TER_gran_BL	None (control)

MTT method

Experiments were conducted using unmodified material and material modified with osteogenon (see table 1). After sterilization, the materials were placed on 96-well plates. A cell suspension (1*104 cells/ml, 0.2 ml per well) was applied to the materialsand was incubated for 24 hours, 1 week, 2 weeks, and 3 weeks at 37 ˚C in 5% CO2. After incubation period, the medium was aspirated, and each well was washed with PBS. MTT mixture for 3 hours at 37 ˚C in 5% CO2. The medium was aspirated, and DMSO with NH3 was added to each well. The DMSO with NH3 in the wells were transferred into a new plate and was measured at 550 nm.

Fluorescence staining

The materials were sterilized and placed into a 24-well plate. Saos-2 cells were seeded on materials at the final concentration 1*105 cells/ml (0.8 ml per well). After 24 h, 1 week or 3 weeks, the medium was aspirated and cells were washed with PBS and stained with 0.01% acridine orange (0.3 ml/well) for 1 minute at dark place. Subsequently the cells were washed 10 times (up to 20x) with PBS. The materials were transferred to microscope slide and observed under the fluorescence microscope.

Statistical analysis

The results of cells viability were reported as a mean ± standard deviation. Statistical analysis was done on program GraphPad Prism 8. The t-test was used to statistically compare viability of cells on modified materials to viability on TER_gran_BL. Comparison was done always between samples of same incubation time. Significant differences were determined under p value 0.05.

3. Results

Figure 1 displays microscopic images of the pure terpolymer (TER_gran_BL) and the terpolymer modified with osteogenon drug (TER_OST_5_BL), taken at 40x, 100x, and 200x magnification. The surface of the pure terpolymer appeared smooth and devoid of inclusions, whereas numerous agglomerates of osteogenon powder were observed in the images of the terpolymer-osteogenon sample, confirming that the drug was incorporated into the microstructure of the sample.

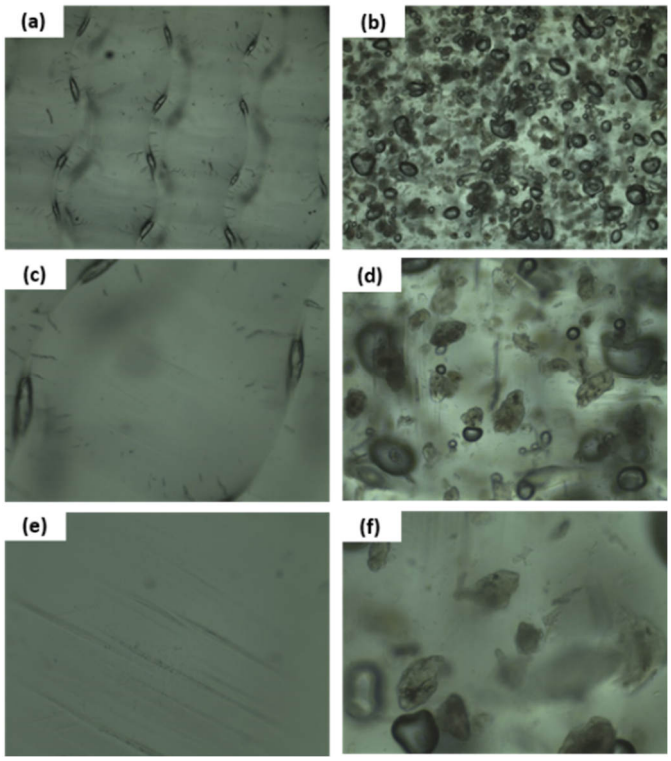

Figure 1: Microscopic images captured with 40x (a,b), 100x (c,d), and 200x (e,f) objective lenses, showing detailed structures of the pure terpolymer (a,c,e) and the terpolymer modified with osteogenon drug (b,d,f)

The Scanning Electron Microscopy (SEM) analysis also confirmed the presence of osteogenon agglomerates within the fabricated samples, providing additional evidence of successful drug incorporation. The SEM image of the pure terpolymer (Figure 2a) shows a smooth surface, while the modified sample (TER_OST_5_BL) reveals visible osteogenon powder agglomerates. EDS spectra (Figure 2d) confirm the presence of characteristic elements associated with the osteogenon drug in the modified sample.

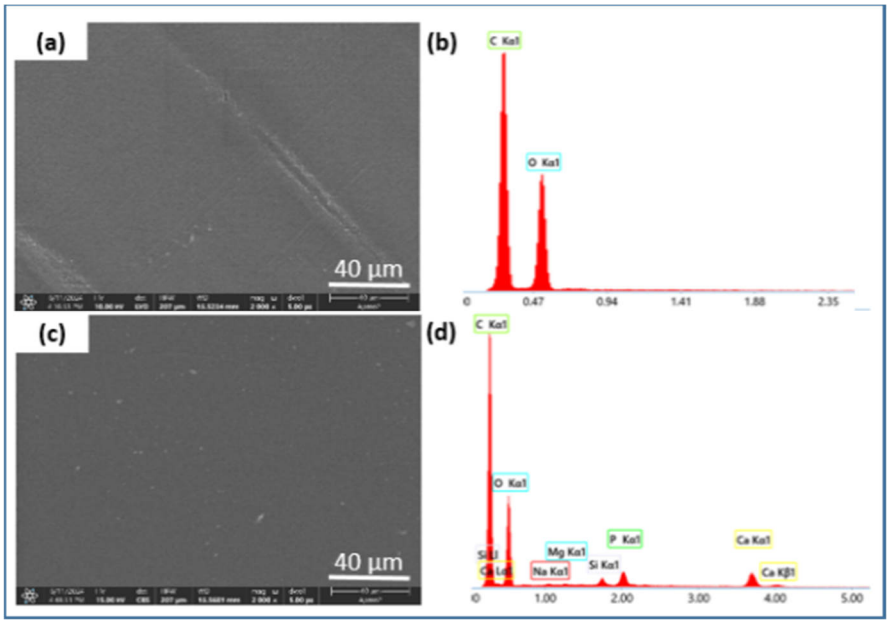

Figure 2: SEM images and EDS analysis of pure terpolymer (a,b) and terpolymer modified with osteogenon drug (c,d), captured at 2000x

The FTIR spectra of the terpolymer poly(L-lactide-co-glycolide-co-caprolactone) and the terpolymer modified with the osteogenon drug are shown in Figure 3. Both spectra reveal characteristic absorption bands corresponding to

the functional groups in the monomers. Distinct bands associated with the C-H stretching vibrations of CH (2995 cm^{-1}) and CH_3 (2945 cm^{-1}) groups are visible. The 1745 cm^{-1} band corresponds to the stretching vibration of the carbonyl (C=O) groups in ester linkages, a common feature in all three monomers: L-lactide, glycolide, and caprolactone. The 1452 cm^{-1} and 1425 cm^{-1} bands are attributed to C-H bending vibrations in -CH_2 groups, primarily from the caprolactone and partially from the glycolide segments. The 1382 cm^{-1} and 1364 cm^{-1} bands represent C-H bending vibrations of -CH_3 groups, which are characteristic of L-lactide. The 1180 cm^{-1} band corresponds to the stretching of C-O and C-O-C bonds in ester groups, typical of the terpolymer. Additionally, the bands at 1128 cm^{-1}, 1084 cm^{-1}, and 1044 cm^{-1} are associated with the stretching vibrations of C-O and C-O-C bonds, particularly in the ester linkages of the caprolactone segments. Collectively, these bands confirm the presence of functional groups from all three monomers.

The FTIR spectrum of the osteogenon sample displayed distinct bands at 1015 cm^{-1} and 557 cm^{-1}, indicating the presence of hydroxyapatite. A shoulder peak at 1634 cm^{-1} marks the position of the amide I band. For collagen in the osteogenon-drug sample, characteristic amide absorption regions are observed, with amide I typically found between 1600–1700 cm^{-1}, primarily due to C=O stretching vibrations in peptide groups. However, no bands related to the osteogenon drug were detected in the composite sample.

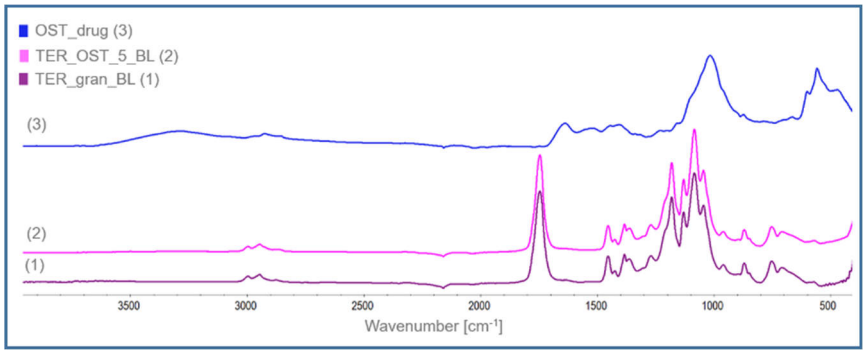

Figure 3: FTIR-ATR spectrum of (3) terpolymer poly(L-lactide-co-glycolide-co-caprolactone); (2) terpolymer modified with osteogenon drug; (3) osteogenon drug

Saos-2 cells were incubated with modified (TER_OST_5_BL) /unmodified (TER_gran_BL) material for 1 day, 1 week, 2 weeks, and 3 weeks at 37°C, 5% CO2. The unmodied material was set as a control. The results of the MTT assay are shown in Figure 4. Cells in contact with TER_OST_5_BL had higher viability than cells on TER_gran_BL after 2 and 3 weeks incubation ($p<0.01$). Cells on materials TER_OST_5_BL showed lower viability than the control after 1 day and 1 week of incubation ($p<0.01$) for one day incubation and $p<0.05$ for 1 week incubation. The highest viability was observed after 3 weeks incubation (114.08 %).

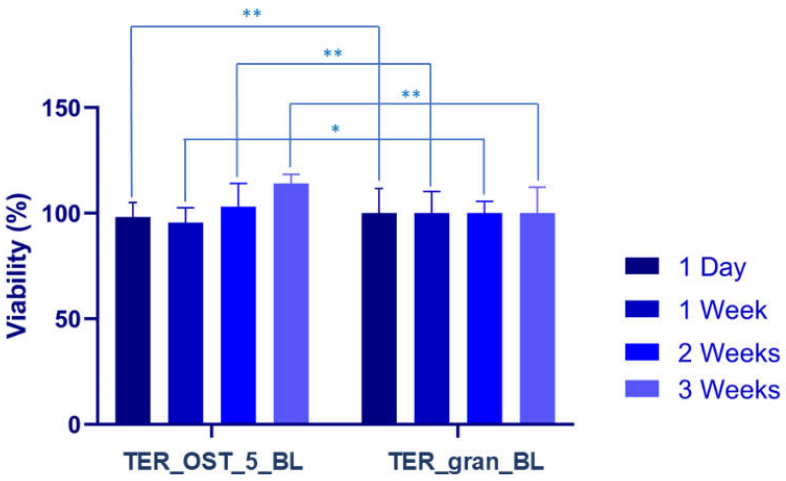

Figure 4: MTT assay of Saos-2 cells. Cells were incubated with TER_OST_5_BL and TER_gran_BL for 1 day, 1 week, 2 weeks, and 3 weeks. Viability was expressed as a percentage of control. Data were shown as mean±SD (n = 3). Statistical analysis was performed by t-test, with the criterion for statistical significance as follows: nonsignificant (ns) at p value > 0.05, significant at $p<0.05$ *, and significant at $p<0.01$ **

Representative images of cells with materials after incubation for 24h, 1 week and 3 weeks obtained with a fluorescence microscope (Figure 5). The amount of living cells (green color) were time dependend. TER_OST_5_BL and TER_gran_BL supported the expansion of viable cells.

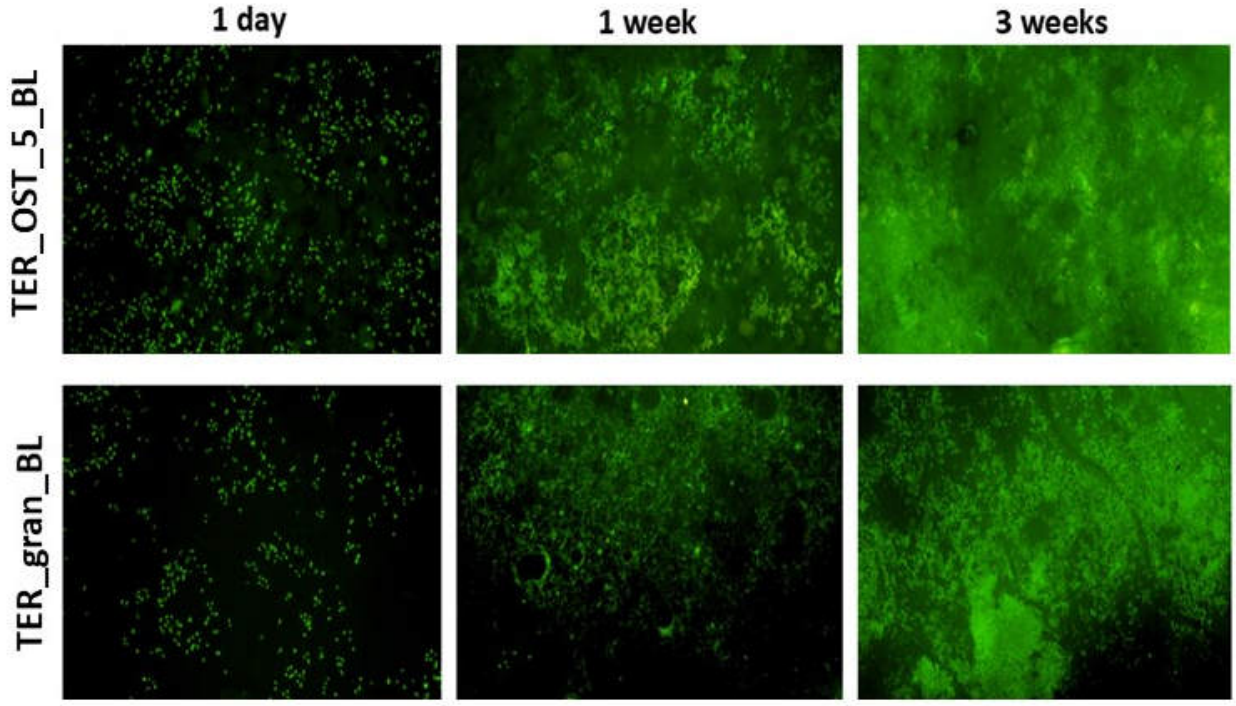

Figure 5: Fluorescent microscopy images of cells cultivated on materials modified with ostegenon (TER_OST_5_BL) and pure materials (TER_gran_BL) after 24 hours, 1 week and 3 weeks at x4 magnification. Cells were stained with acridine orange (green color, viable cells). (n=3)

The recorded deformations of the samples at selected moments in time are shown in Figure 6. Figure 7 shows the measured angular values of deformations from the temporary shape after triggering the process of returning to the original shape.

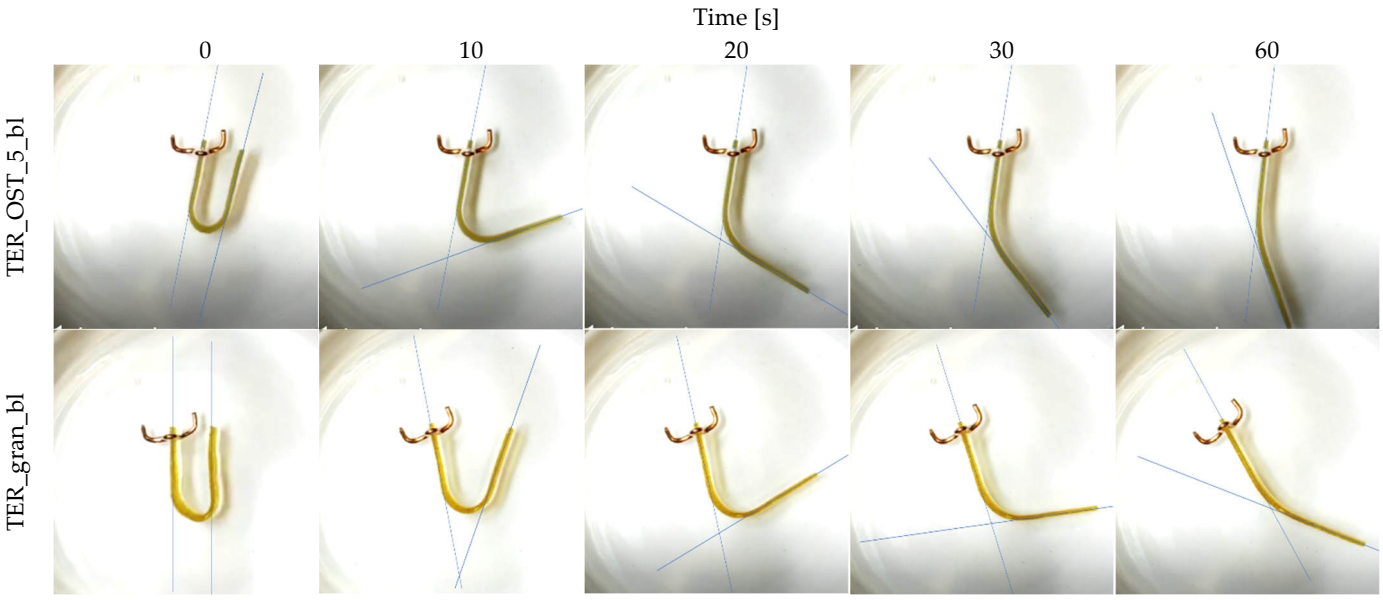

Figure 6: Photos of samples returning to their original shape

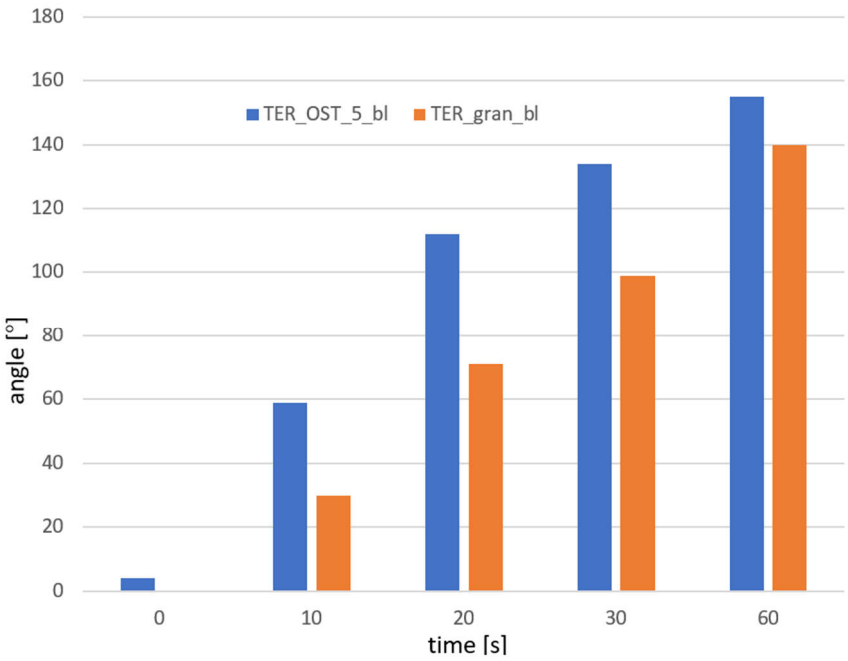

Figure 7: Deformation angle of temporary samples

4. Conclusion

The successful incorporation of osteogenon into the poly(L-lactide-co-glycolide-co-caprolactone) terpolymer was confirmed through microscopic and EDS analyses. FTIR analysis revealed the characteristic functional groups of the terpolymer; however, the osteogenon content in the sample was relatively low, resulting in weaker characteristic bands that were overshadowed by the intense signals from the terpolymer matrix. Biocompatibility studies demonstrated that the osteogenon-modified terpolymer (TER_OST_5_BL) promotes higher cell viability over time compared to the unmodified sample, particularly after extended incubation, indicating enhanced support for cellular proliferation. These findings suggest that the osteogenon-modified terpolymer holds significant promise for 4D printing of medical implants, offering a bioactive, adaptable material that supports cellular integration and meets the evolving demands of biomedical applications. Shape memory tests showed an increased ability to return to the original shape of samples made of osteogenone-modified terpolymer (TER_OST_5_BL) compared to samples made of unmodified terpolymer.

Acknowledgments

This project was supported by grants: Grant Agency of the Czech Republic (GAČR 21-45449L), internal Grant Agency of the Faculty of Medicine, Palacky University Olomouc (IGA_LF_2024_011) and by the National Science Centre, Poland, in the frame of the project "3D and 4D printing of stimuli-responsive and functionally graded biomaterials for osteochondral defects regeneration," grant number: 2020/39/I/ST5/00569 (OPUS-LAP).

Reference

1. S. Amukarimi, Z. Rezvani, N. Eghtesadi, M. Mozafari. Smart biomaterials: From 3D printing to 4D bioprinting. Methods 2022; 205: 191-199, https://doi.org/10.1016/j.ymeth.2022.07.006
2. F. Demoly; M.L. Dunn; K.L Wood, H.J Qi, J.C. André. The status, barriers, challenges, and future in design for 4D printing. Materials & Design 2021; 212: 110193. https://doi.org/10.1016/j.matdes.2021.110193
3. S. Jolaiy, A. Yousefi, M. Hosseini, A. Zolfagharian, F. Demoly, M. Bodaghi. Limpet-inspired design and 3D/4D printing of sustainable sandwich panels: Pioneering supreme resiliency, recoverability and repairability. Applied Materials Today 2024; 38: 102243. https://doi.org/10.1016/j.apmt.2024.102243

4. H. Doostmohammadi, K. Kashmarizad, M. Baniassadi, M. Bodaghi, M. Baghani. 4D printing and optimization of biocompatible poly lactic acid/poly methyl methacrylate blends for enhanced shape memory and mechanical properties. Journal of the Mechanical Behavior of Biomedical Materials 2024; 160: 106719. https://doi.org/10.1016/j.jmbbm.2024.106719
5. P. Kumar, P. Suryavanshi, S. Kumar Dwivedy, S Banerjee. Stimuli-responsive materials for 4D Printing: Mechanical, Manufacturing, and Biomedical Applications. Journal of Molecular Liquids 2024; 410: 125553, https://doi.org/10.1016/j.molliq.2024.125553
6. K. Hashimoto, N. Kurokawa, A. Hotta. Controlling the switching temperature of biodegradable shape memory polymers composed of stereocomplex polylactide / poly(d,l-lactide-co-ε-caprolactone) blends. Polymer 2021; 233: 124190, https://doi.org/10.1016/j.polymer.2021.124190
7. F. Pilate, A. Toncheva, P. Dubois, J.M. Raquez. Shape-memory polymers for multiple applications in the materials world. European Polymer Journal 2016; 80: 268–294, http://dx.doi.org/10.1016/j.eurpolymj.2016.05.004
8. E. Pamuła, P. Dobrzynski, M. Bero, C. Paluszkiewicz. Hydrolytic degradation of porous scaffolds for tissue engineering from terpolymer of L-lactide, ε-caprolactone and glycolide. Journal of Molecular Structure 2005; 744–747: 557–562
9. A. Bajpai, A. Baigent, S. Raghav, C.O. Brádaigh, V. Koutsos, N. Radacsi. 4D Printing: Materials, Technologies, and Future Applications in the Biomedical Field. Sustainability 2020, 12, 10628. https://doi.org/10.3390/su122410628
10. I. Rajzer, E. Menaszek, O. Castano. Electrospun polymer scaffolds modified with drugs for tissue engineering. Materials Science and Engineering: C 2017; 77: 493-499, https://doi.org/10.1016/j.msec.2017.03.306